Neurophysiological Evidence for a Traveling Wave in the Amphibian Inner Ear

Abstract. *In response to low-frequency sounds (less than 1.0 kilohertz) auditory nerve fibers in the treefrog,* Eleutherodactylus coqui, *discharge at a preferred phase of the stimulus waveform which is a linear function of the stimulus frequency. Moreover, the slopes of the phase-versus-frequency functions (equivalent to the system time delays) systematically increase as the characteristic frequency of the fibers decreases. These neurophysiological observations, coupled with the known tonotopy of the amphibian papilla suggest that a traveling wave occurs in the inner ear of frogs despite the absence of a basilar membrane. Electrical tuning may contribute to these characteristic frequency–dependent delays.*

The inner ear of amphibians is a complex structure unique among vertebrates. Anurans (frogs and toads) have two distinct auditory organs, the amphibian papilla (AP) and basilar papilla. Neither organ contains a basilar membrane; rather, shearing forces between hair cells and the overlying tectorial membrane (TM) result from the movement of the surrounding fluid and TM relative to the stationary hair cell receptors (*1, 2*). Despite this unique inner ear morphology, anuran auditory nerve fibers show frequency selectivity similar to that in other vertebrates and display a tonotopic arrangement of the receptor cells in the AP (*3–5*). The tonotopy of this organ may result in part from a spatial gradation of mass in the TM (*4, 6*). The most massive TM region overlies the rostral end of the papilla, which is innervated by fibers with low characteristic frequencies (CF's of less than 0.3 kHz), whereas the least massive region of the TM is associated with the caudal end of the papilla, which is innervated by high-frequency fibers (CF's of 0.5 to 1.0 kHz).

It has been unclear whether the TM could support a traveling wave in a manner analogous to the basilar membrane of birds and mammals. Our phase-frequency measurements of auditory nerve responses now provide physiological evidence for the propagation of such a mechanical disturbance in the AP of the anuran inner ear and thus strongly implicate the TM as the structure supporting such a wave. Measurements of the cumulative phase shift of spike occurrence with increasing stimulus frequency allow us to estimate the time required for the stimulus waveform to travel from the animal's tympanum to the receptor. From the systematic inverse relation between travel time and CF we infer the pathway for hair-cell stimulation and provide direct support for the notion of a traveling wave in the AP.

We studied the phase-locking ability of 53 auditory nerve fibers in 11 adult treefrogs, *Eleutherodactylus coqui*, for stimulus frequencies between 0.05 and 1.1 kHz. After immobilizing the frogs, (*d*-tubocurarine chloride) and applying a topical anesthetic (Lidocaine), we used a ventral surgical approach to expose the eighth nerve and isolate single auditory neurons with conventional glass micropipettes. Monaural stimuli were generated by a beat-frequency oscillator (Bruel & Kjaer 2010), presented to the animal through an earphone (Beyer DT-48) coupled to a closed acoustic delivery system and monitored with a microphone (Bruel & Kjaer 4134). An automated threshold tracking routine was used to determine a tuning curve for each neuron studied (*7*).

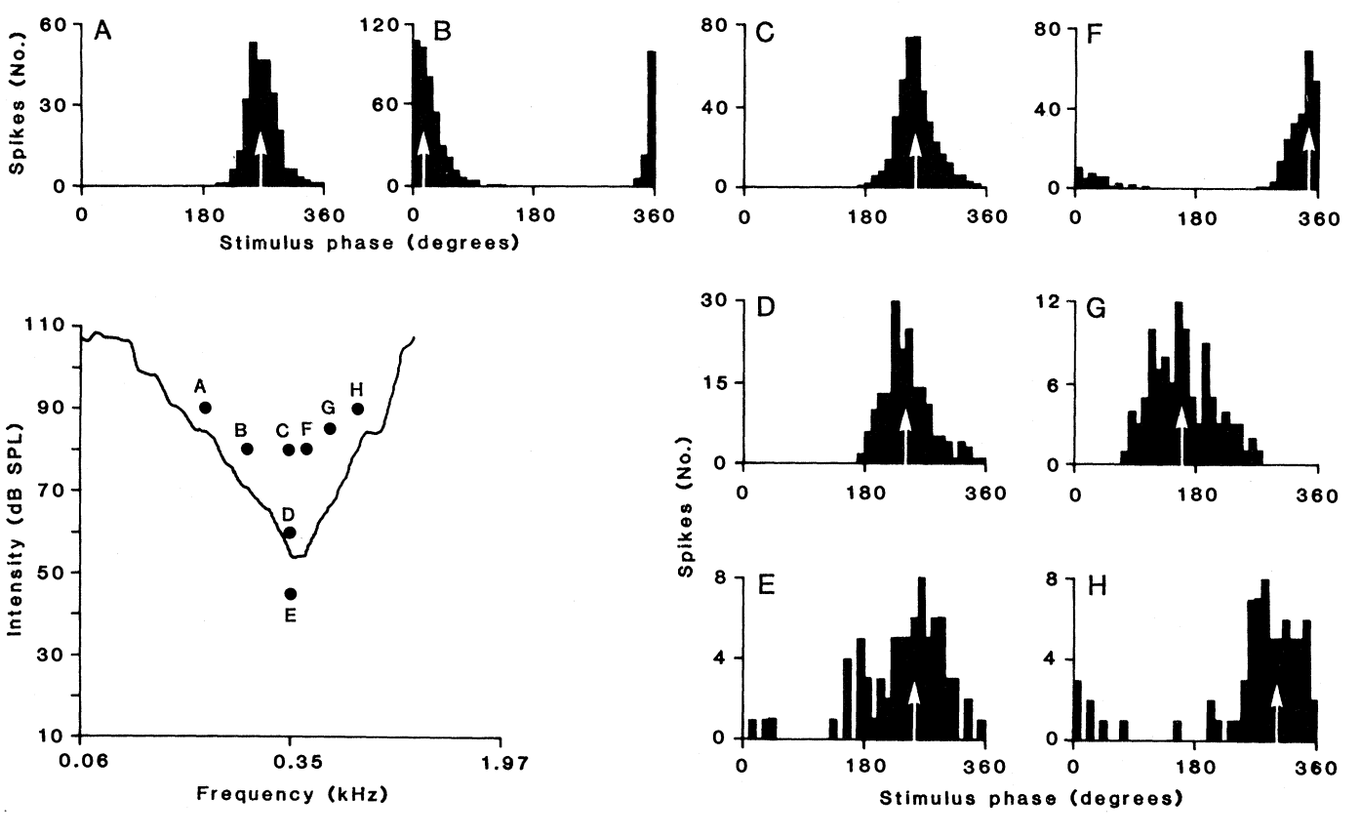

Fig. 1. (Lower left) Tuning curve for an AP fiber with CF = 0.36 kHz at 53 dB sound pressure level (SPL). (A–H) Period histograms were recorded for this neuron in response to continuous tones (1.4 to 20 seconds duration). Bin width for each histogram is 10°. The mean phase angle (θ) for each (white arrow) shifts systematically to the right with stimulus frequency. Stimulus frequency and preferred firing phase: (A) 0.18 kHz, 268°; (B) 0.25 kHz, 17°; (C–E) 0.35 kHz, 241° to 254°; (F) 0.40 kHz, 343°; (G) 0.50 kHz, 159°; and (H) 0.60 kHz, 303°.

Details of these techniques have been published (*5*). Period histograms were generated through the use of the positive zero crossing of the stimulus waveform to trigger a fast data acquisition unit (Cambridge Electronic Design, model 502), which marked the occurrence of each action potential with reference to a single cycle of the stimulus frequency. Before each experiment, and at each frequency, the stimulus generation system was calibrated to correct for any phase shifts introduced by our equipment (*8*). For each period histogram we measured the stimulus frequency and intensity, the number of spikes evoked, the mean preferred phase angle (θ), and the vector strength (*VS*), which is a quantitative measure of the synchronization of the discharges to a particular phase of the stimulus (*9*).

The period histograms collected from a single neuron (Fig. 1) demonstrate that the degree of phase locking increases rapidly with stimulus level (Fig. 1, C, D, and E) until the stimulus is 0 to 10 dB above the discharge rate threshold, at which point *VS* saturates. Significant phase locking to stimulus frequencies 10 to 15 dB below the tuning curve threshold was not uncommon. The relationship between the mean response phase and stimulus frequency was studied with test frequencies separated by 10 to 100 Hz to ensure that the resulting phase shift increment would be less than 2π. We found that the mean response phase systematically increased (phase lag) with stimulus frequency (Fig. 1, A, B, C, F, G, and H). Cumulative phase angle (expressed in radians) showed a linear relationship with stimulus frequency (Fig. 2A) in all neurons examined (*10*); it is thought to reflect a constant delay interposed between the stimulus and neural response (*11*).

We estimated the delay occurring in this system by measuring the rate at which phase accumulates with stimulus frequency (f). The slope of each function ($d\theta/df$) was inversely proportional to the neuron's CF (Fig. 2B). The decreasing slope of the phase-frequency functions with increasing CF is interpreted as a time delay ($d\theta/2\pi df$) between stimulus onset and the recorded neural response that is greatest for fibers with low CF's (*12*). The transmission time of the middle ear is small and roughly constant over the frequency range of interest (*13*). Thus, any differences in the travel time estimates for particular receptors result from differential time to neural excitation via the fluid–TM–hair cell pathway and from propagation time required for the action potential to reach the recording electrode. These values (minus neural delay) are plotted in Fig. 2C (*14*). Coupled with the known tonotopic arrangement of hair cells (*4*), these travel time differences suggest that a mechanical disturbance moves progressively along the caudal to rostral axis of the AP, first stimulating neurons with high CF's and later reaching those with low ones.

We have considered alternative models to explain the CF-dependent time delays. Whereas in reptiles tonotopy is derived from the micromechanical properties of the stereocilia (*15*), the observed gradations in cilia height of the anuran AP show no correspondence to its tonotopic map (*16*) and therefore do not correspond to the CF-dependent time delays we observed. Recently, electrical tuning of hair cell receptors has been documented in the turtle (*17*) and proposed for the bullfrog sacculus (*18*). In theory, a portion of the CF-dependent delays reported here could arise from the filter characteristics of such tuned receptors. However, the neural tuning curve bandwidths predict delays much longer than those we measured (*19*).

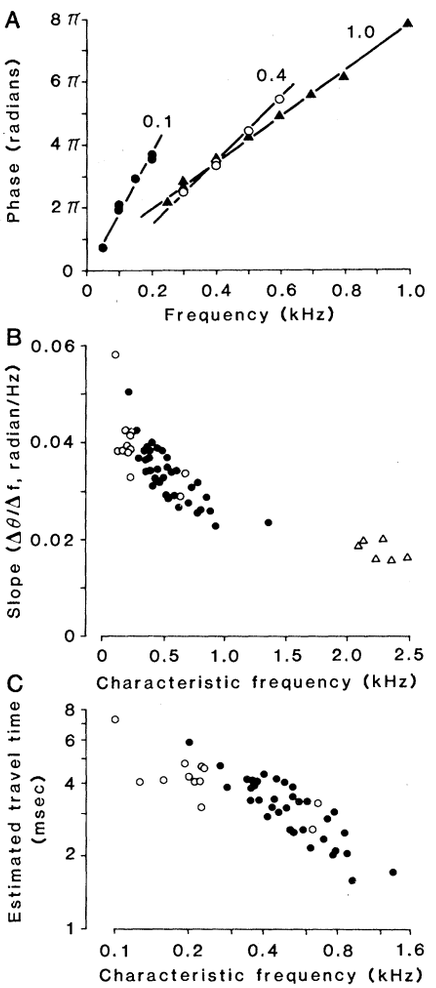

Fig. 2. (A) Cumulative phase shift with different stimulus frequencies for three representative AP fibers in one animal. The CF for each unit is shown. (B) Slope of the least squares fit for each fiber as a function of CF (n = 53). These measures can be converted to a measure of total delay (in seconds) by multiplying by $1/2\pi$. ●, Amphibian papilla neurons, $R^2 \geq 0.98$; ○, AP neurons, $0.89 \leq R^2 < 0.98$; △, basilar papilla neurons. (C) Estimated travel time calculated from the slope of the phase/frequency functions is plotted against CF in log-log format to facilitate comparison of similar plots for mammalian data (*11*). Those data points derived from regression fits to the phase/frequency data with $R^2 < 0.98$ are indicated by open circles. The average neural delay [estimated to be 2.0 msec (*14*)] has been subtracted from all measurements. The range of travel times for AP fibers was 1.5 to 7.3 msec.

In a previous analysis of the phase-frequency relations in the squirrel monkey (*11*) a logarithmic relationship between travel time and CF was described similar to the relation we observed for the treefrog. This is remarkable in light of the very different morphologies of the inner ear of anurans and mammals. In the mammalian auditory system this relationship results from a traveling wave in the cochlea, the tonotopic arrangement of the mammalian hair cells and the logarithmic association between hair cell CF with position along the cochlea (*20*). The interaction between the fluid mass of the inner ear and the cochlear partition compliance allows the propagation of the low-velocity (relative to the bulk propagation velocity of the fluid) traveling wave on the mammalian basilar membrane. Frogs lack a basilar membrane, and yet our physiological results demonstrate CF-dependent time delays consistent with a low-velocity mechanical disturbance (traveling wave), supported by the TM in the anuran AP (*21*). The physical mechanisms underlying the generation of this traveling wave on the TM are not understood. Direct mechanical measurements are now needed to determine the dynamic properties of the TM in response to sound.

CYNTHIA M. HILLERY
PETER M. NARINS
Department of Biology, University of California, Los Angeles 90024

References and Notes

1. C. D. Geisler, W. A. van Bergeijk, L. S. Frishkopf, *J. Morphol.* **114**, 143 (1964); R. E. Lombard, in *Comparative Studies of Hearing in Vertebrates*, A. N. Popper and R. R. Fay, Eds. (Springer-Verlag, New York, 1980), pp. 121–138.
2. E. G. Wever, *J. Morphol.* **141**, 461 (1973); in *Handbook of Sensory Physiology*, vol. 5, *Auditory System*, part 1, *Anatomy, Physiology (Ear)*, W. D. Keidel and W. D. Neff, Eds. (Springer-Verlag, Berlin, 1974), pp. 423–454; R. R. Capranica, in *Frog Neurobiology*, R. Llinas and W. Precht, Eds. (Springer-Verlag, Berlin, 1976), pp. 551–575.
3. A. S. Feng, P. M. Narins, R. R. Capranica, *J. Comp. Physiol.* **100**, 221 (1975).
4. R. R. Capranica and A. J. M. Moffat, *J. Acoust. Soc. Am.* **62**, S36 (1977); E. R. Lewis, E. L.

Leverenz, H. Koyama, *J. Comp. Physiol.* **145**, 437 (1982); E. R. Lewis, R. A. Baird, E. L. Leverenz, H. Koyama, *Science* **215**, 1641 (1982); E. R. Lewis and E. L. Levernz, *Scanning Electron Micros.* **1983-1**, 189 (1983).
5. P. M. Narins and C. M. Hillery, in *Hearing—Physiological Bases and Psychophysics*, R. Klinke and R. Hartmann, Eds. (Springer-Verlag, Berlin, 1983), pp. 70–76.
6. E. R. Lewis, *Neurosci. Lett.* **21**, 131 (1981); W. P. Shofner and A. S. Feng, *Hearing Res.* **11**, 103 (1983).
7. Tuning curve threshold was determined by the standard mammalian testing procedure [N. Y. S. Kiang, E. C. Moxon, R. A. Levine, in *Sensorineural Hearing Loss*, G. E. W. Wolstenholme and J. Knight, Eds. (Churchill, London, 1970), pp. 241–273; M. C. Liberman, *J. Acoust. Soc. Am.* **63**, 442 (1978)]. We compared the number of spikes occurring during a 50-msec test tone and a 50-msec control period. The intensity was adjusted in ±1-dB steps until the stimulus tone consistently evoked one more spike than occurred spontaneously. This intensity level was defined as threshold and corresponded to a spike discharge rate equal to 20 spikes per second above the spontaneous rate.
8. We measured the phase shift between the electrical signal that triggered data acquisition and the stimulus at the animal's tympanum with a calibrated nose cone–probe tube microphone assembly and a high-resolution timer-counter (Phillips PM6671). This phase shift was added to the phase angles measured relative to the input to the zero-crossing detector to obtain the phase angle of the stimulus at the animal's tympanum.
9. J. M. Goldberg and P. B. Brown, *J. Neurophysiol.* **32**, 613 (1969). For strong phase locking, *VS* approaches a value of 1.0 and the period histograms show a tightly peaked distribution. To test whether the spike distribution of a period histogram differed significantly from a random distribution, we determined the likelihood value $(L) = 2n(VS)^2$, in a Rayleigh test of circular data where n is the number of spikes counted [K. V. Mardia, *Statistics of Directional Data* (Academic Press, London, 1972), pp. 133–138]. The null hypothesis (no phase locking) is a uniform distribution of events.
10. $0.89 \leq R^2 \leq 0.99$, $n = 53$. On the average a fiber was stimulated with 10 to 15 test frequencies; range, 4 to 37. Slope values (rad/Hz) for AP fibers ranged from 0.0228 to 0.0583. To a first approximation, phase lag seems to be a linear function of frequency. To the extent that these functions are linear, $d\theta/2\pi df$ is a measure of the system delay. In mammals, however, the rate of phase accumulation above CF may depend on frequency; hence, mammalian travel times calculated from a regression line through the phase-frequency data may be overestimated. [R. R. Pfeiffer and C. E. Molnar, *Science* **167**, 1614 (1970); M. A. Ruggero, *J. Acoust. Soc. Am.* **67**, 707 (1980); D. D. Greenwood, unpublished]. In 23 percent of the neurons we examined, slight deviations from linearity were detected that reduced the goodness of a single linear fit to these data ($0.89 \leq R^2 \leq 0.97$) when compared with the remainder of the fibers ($0.98 \leq R^2 \leq 0.99$). These neurons are indicated by open circles in Fig. 2, B and C. Most of the "nonlinear" fibers had CF's of less than 0.23 kHz. These units, which derive from hair cells at the rostral end of the papilla beneath the most massive portion of the tectorium, may be subject to more mechanical nonlinearities (edge effects, mechanical reflections). Estimates of delay for low CF units are therefore subject to greater variability. For these cases, the rate of phase accumulation was less at higher stimulus frequencies.
11. D. J. Anderson, J. E. Rose, J. E. Hind, J. F. Brugge, *J. Acoust. Soc. Am.* **49**, 1131 (1971).
12. Figure 2B includes data for six neurons from the basilar papilla, with CF's between 2.1 and 2.5 kHz. These fibers showed smaller phase accumulations with increasing stimulus frequency than did AP fibers. This observation supports the notion of a short delay and direct route (*2*) for the stimulus disturbance to reach the basilar papillar cells relative to AP cells.
13. J. C. Saunders and B. M. Johnstone, *Acta Oto-Laryngol.* **73**, 353 (1972); A. J. M. Moffat and R. R. Capranica, *J. Comp. Physiol.* **127**, 97 (1978).
14. The average neural plus middle-ear delay was estimated to be 2.0 msec [P. M. Narins, thesis, Cornell University (1976)] and corresponds to the shortest latencies of responses measured to clicks by high-frequency units.
15. R. G. Turner, A. A. Muraski, D. W. Nielsen, *Science* **213**, 1519 (1981); T. Holton and A. J. Hudspeth, *ibid.* **222**, 508 (1983).
16. E. R. Lewis, *Brain Behav. Evol.* **13**, 196 (1976); *Scanning Electron Microscopy* **2**, 429 (1977); ——— and E. L. Leverenz, *Abstr. ARO Res. Mtg.* **6**, 99 (1983).
17. A. C. Crawford and R. Fettiplace, *J. Physiol. (London)* **306**, 79 (1980); *ibid.* **312**, 377 (1981); R. Fettiplace and A. C. Crawford, *Hearing Res.* **2**, 447 (1980).
18. R. S. Lewis and A. J. Hudspeth, in *Hearing—Physiological Bases and Psychophysics*, R. Klinke and R. Hartmann, Eds. (Springer-Verlag, Berlin, 1983), pp. 17–24.
19. Under the most general conditions, the response time for a tuned filter is inversely proportional to its bandwidth. The bandwidths of AP hair cells are not known, but may be estimated from neural bandwidths at 3 dB above best threshold (BW_{3dB}). Using response time (RT) = $1/BW_{3dB}$, which is related to delay through a tuned filter, we determined the predicted RT's for each unit. These estimates were as much as 19 msec longer than the values we observed. Further, cells with the same bandwidths often had time delays that differed by as much as 3 msec. Such variation would not be predicted if the cells act like simple electrical filters. Although the mean difference between the estimated RT and the observed time delays was 8.6 ± 0.87 msec, the former did show a weak inverse relation to CF. Investigations of the electrical characteristics of AP hair cells are required before we can effectively evaluate whether electrical tuning properties contribute significantly to the observed delays.
20. H. F. Schuknecht, *Arch. Otolaryngol.* **58**, 377 (1963); D. D. Greenwood, *J. Acoust. Soc. Am.* **33**, 484 (1962); in *Sensation and Measurement*, H. R. Moskowitz, B. Scharf, J. C. Stevens, Eds. (Reidel, Dordrecht, 1974), pp. 231–239.
21. The TM is implicated in this system since it may generate and propagate intermodulation distortion products [R. R. Capranica and A. J. M. Moffat, in *Comparative Studies of Hearing in Vertebrates*, A. N. Popper and R. R. Fay, Eds. (Springer-Verlag, New York, 1980), pp. 139–165] and participate in the active process of tone generation associated with spontaneous and evoked acoustic emissions from the ear of *Rana esculenta* [A. R. Palmer and J. P. Wilson, *J. Physiol. (London)* **324**, 66P (1981)].
22. Supported by NIH grants NS07005-02 and NS 19725-01 to C.M.H. and P.M.N., respectively. Special thanks are due R. Dunia for assistance with the experiments, C. B. Martinez for developing the phase analysis program, R. D. Zelick for critical input during all phases of this study, and especially E. R. Lewis and W. G. Sokolich for enlightening discussions and suggestions.

9 January 1984; accepted 18 June 1984

Enhanced Arboviral Transmission by Mosquitoes That Concurrently Ingested Microfilariae

Abstract. *Infection, dissemination, and transmission of an arbovirus in mosquitoes are enhanced by concurrent ingestion of microfilariae. Ingestion of Rift Valley fever virus alone infected only 64 percent of female* Aedes taeniorhynchus. *Of these, only 5 percent of refeeding mosquitoes actually transmitted virus. In contrast, ingestion of the same amount of virus from concurrently microfilaremic (*Brugia malayi*) gerbils resulted in 88 percent infection and 31 percent transmission. Enhanced transmission of virus may be attributed to increased transit of virus across the midgut wall. Endemic filariasis may promote arbovirus transmission in nature.*

Viral transmission by an arthropod requires that the virus infect cells of the midgut and pass into the hemocoel in order to infect the salivary glands. Failure of western equine encephalomyelitis virus to disseminate across the gut wall in a percentage of *Culex tarsalis* limits this species as a vector of the virus (*1*). Similarly, the failure of virus to disseminate in a percentage of *Culex pipiens* limits this species as a vector of Rift Valley fever (RVF) virus (*2*). Any factor that allows virus to directly enter the hemocoel could result in increased competence of a vector for that virus. For example, Merrill and TenBroek (*3*) found that female *Aedes aegypti* that had ingested eastern equine encephalomyelitis (EEE) virus did not transmit the virus by bite. However, if virus were inoculated, or if the midgut were punctured immediately after ingestion of EEE virus, this species was able to transmit EEE virus by bite. Perhaps the punctures allow virus to disseminate into the hemocoel directly. A similar finding was reported for *Anopheles annulipes* and Murray Valley encephalitis virus (*4*).

Because microfilariae ingested in a blood meal rapidly penetrate the mosquito midgut, they may facilitate viral infection and dissemination to remote organs of the vector. Also, injected virus becomes transmissible more rapidly than does ingested virus (*5*). Thus we hypothesized that mosquitoes fed on a host concurrently viremic and microfilaremic would transmit virus more effectively than mosquitoes fed on a host infected with virus alone. We therefore permitted *Aedes taeniorhynchus* to ingest blood from gerbils (*Meriones unguiculatus*) concurrently infected with *Brugia malayi* and RVF virus. Infection, hemocoelic dissemination, transmission rates, and duration of preinfectious period were compared to those of mosquitoes ingesting virus alone.

In the first experiment (*6*), we compared the rapidity of virus dissemination in the mosquitoes that ingested RVF virus (*7*) alone with that in the mosquitoes ingesting virus and *B. malayi* microfilariae (*8*) concurrently. Each mosquito ingested approximately $10^{3.3}$ plaque-forming units of RVF virus from one of two gerbils. The mosquitoes that fed on the gerbil with concurrent microfilaremia ingested in addition a median of 85 microfilariae. After ingestion of virus alone, 59 percent of 85 *Ae. taeniorhynchus* became infected (Table 1). Of the